Melting-Induced Enhancement of the Second-Harmonic Generation from Metal Nanoparticles

A. M. Malvezzi,[1] M. Allione,[2] M. Patrini,[2] A. Stella,[2] P. Cheyssac,[3] and R. Kofman[3]

[1]*INFM and Dipartimento di Elettronica, Università di Pavia, Via Ferrata 1, I-27100 Pavia, Italy*

[2]*INFM and Dipartimento di Fisica "A. Volta," Università di Pavia, Via Bassi 6, I-27100 Pavia, Italy*

[3]*LPMC, UMR 6622, Universitè de Nice-Sophia Antipolis, 06108 Nice Cedex 2, France*

(Received 18 December 2001; published 2 August 2002)

We report on the generation of second-harmonic signals by irradiating monolayers of high purity Ga nanoparticles, embedded in a SiO_x matrix, with femtosecond laser pulses at 800 nm. A remarkable melting-induced enhancement of the second-harmonic generation is observed in correspondence of the phase transition. In addition, the hysteresis cycle of nonlinear transmittance is shown to be amplified a factor of 80–100 with respect to the linear response and interpreted in the framework of a nonlinear effective-medium model.

DOI: 10.1103/PhysRevLett.89.087401 PACS numbers: 78.67.Bf, 42.65.Ky, 61.25.Mv, 78.66.Vs

From the first observations and comprehensive theory of nonlinear optical phenomena developed in the early 1960s the number of systems and methods for generating nonlinear effects and, in particular, second-harmonic signals from solid surfaces has considerably increased [1]. In the 1970s, one-order-of-magnitude enhancement of surface second-harmonic generation was obtained through excitation of the surface plasmon resonance in silver [2]. In the next decades, the ability to control and grow metal nanoparticles embedded in dielectric matrices has provided structures maximizing the surface-to-volume ratio, which further enhances the nonlinear response [3]. While considerable efforts have been mainly focused on selection of new materials and fabrication techniques, in this work we adopt a different approach by studying the effect of melting (and more generally of phase transitions) on nonlinear optical phenomena in metallic nanoparticles. We observe a remarkable melting-induced enhancement of the second-harmonic signal generated at the phase transition in gallium nanoparticles. We further find that hysteresis cycles of nonlinear transmittance versus temperature across the phase transition are amplified up to a factor of 80–100 with respect to the linear ones.

The generation of second-harmonic radiation, which is generally forbidden in centrosymmetric systems due to symmetry constraints, is enhanced by the excitation of surface plasmons in relatively large metallic nanoparticles (of the order of 5–50 nm radius) involving the participation of higher order multipoles. In order to study the effect of the phase transition on the second-harmonic generation (SHG) we choose the following as starting points: (i) to use gallium, which is expected to yield a large nonlinear response as compared to other metals [4]; (ii) to perform measurements on nanoparticles in which the surface-to-volume ratio for a given amount of active material increases with decreasing particle size; and (iii) to work in resonance with the surface plasmon (SP) peak, as determined by linear optical measurements.

In this work we irradiate monolayers of high purity Ga nanoparticles, embedded in a SiO_x matrix, with femtosecond laser pulses at 800 nm. We measure the generated SH signals as a function of the nanoparticle radius from 2 to 100 nm, and we find for 30 nm an enhancement of the SH generation in correspondence with the resonance with the SP wavelength. Measurements are then repeated as a function of sample temperature from liquid-nitrogen temperature (LNT) to 320 K and back. The observed hysteresis behavior of the SH signal is interpreted in terms of solidification and melting of the nanoparticles, through a model which accounts for the increased SH generation in the liquid phase.

The samples are grown by evaporation condensation (Vollmer-Weber mode) of high purity gallium in ultrahigh vacuum [5] over a dielectric SiO_x ($x \sim 1$) layer deposited on a silica or sapphire substrate. Because of the partial wetting character of Ga with respect to SiO_x (the contact angle being 130° [6]), the formation of Ga nanodroplets occurs on the substrate at a temperature around the melting point of bulk Ga ($\sim$300 K). Liquid nanoparticles with the shape of truncated spheres are then solidified by cooling the substrate down to LNT, and they keep the same shape. The crystalline structure of the solid nanoparticles is a mixture of β and δ metastable phases, as determined by high-resolution transmission electron microscopy measurements [7]. A SiO_x layer evaporated over the surface stabilizes the nanoparticle distribution and avoids ambient contamination. The average size turns out to be a linear function of evaporation time at constant deposition rate. Both size and size dispersion (20% of the nominal value) are determined by means of electron microscopy [5,8]. The second-harmonic radiation is measured in transmission and reflection with a femtosecond Ti:sapphire laser at 800 nm, repetition rate 1 kHz, and pulse duration 150 fs. The maximum pulse fluence on the sample is 5×10^{-3} J/cm^2 at the 0.9 mm diameter focal spot of the 4 m focusing lens used in the experiment. These fluence levels are sufficiently low as to prevent any damage on nanoparticles even after long exposure to laser radiation. The SH signal travels through a combination of color and interference filters and is detected by a photomultiplier.

Temperature measurements are performed by keeping the sample in a cold finger cryostat driven by a temperature controller in the range LNT—320 K with a scan rate of ~2 K/min. Absolute calibration of the measured SH values is obtained by taking into account geometry, optical characteristics of the experimental setup, and detector sensitivity [9]. The nonlinear radiation is spatially coincident with the pump in reflection and transmission.

A detailed analysis of the linear absorbance measured on the samples [8] shows the surface plasmon peak, shifting towards short wavelengths with decreasing particle size, as shown in Fig. 1. From these measurements we observe that the 400 nm wavelength of the SH beam generated by the laser resonates with the SP peak for particle radii $R =$ 20–25 nm. We expect therefore maximum SH emission for these values of R.

Nonlinear reflection $R_{\mathrm{nl}} = I_R(2\omega)/[I_0(\omega)]^2$ and transmission $T_{\mathrm{nl}} = I_T(2\omega)/[I_0(\omega)]^2$ measurements presented in Fig. 2 were performed on several sets of Ga nanoparticle samples at variable fluence levels with linear pump polarization. Here I represents the incident (0), reflected (R), and transmitted (T) fluences at the indicated frequencies. The SH signals follow a quadratic law versus the input flux (see the inset of Fig. 2). Maximum values of R_{nl} and T_{nl} are in the $(2–5) \times 10^{-21}$ cm^2/W range [10]. Substrates, bare as well as covered with SiO_x layers, show negligible SH generation in both reflection and transmission.

SHG signals show a strong dependence on particle size from 2 to 100 nm (Fig. 2). R_{nl} and T_{nl} have approximately the same dependence and reach comparable values. Both intensity measurements exhibit a broad maximum occurring for radii in the range 20–40 nm, and confirm the occurrence of SH enhancement at the spectral coincidence with the SP resonance. The out-of-resonance values are measured to decrease gradually to zero on both sides. A similar behavior is also observed in the SH values measured at LNT.

In a second set of measurements the temperature variation of the SH signal in the range 77–320 K has been recorded for several samples. This is in order to evaluate the nonlinear properties across the solid-to-liquid phase transition of Ga nanoparticles. In bulk and continuous thin films, linear reflectance measurements vs temperature show a complete hysteresis cycle of solidification and melting, the former occurring at ~270 K and the latter at ~300 K [11]. In the case of nanoparticles, it is known that space confinement produces crystalline phases different from the α phase of the bulk Ga. These phases have lower melting and solidification temperatures and a wider hysteresis [12]. Moreover, the size effect adds an additional lowering to these transition temperatures.

For each thermal cycle the samples have been initially heated to 320 K. While continuously measuring the SH

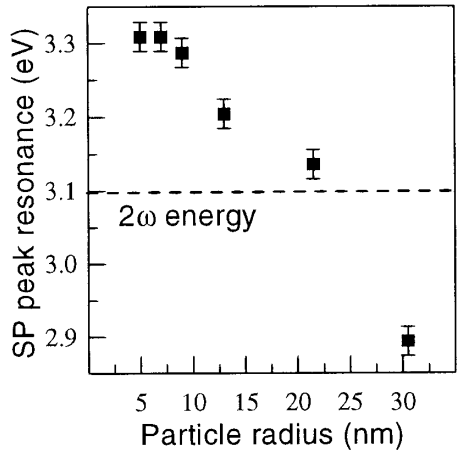

FIG. 1. Position in energy of the surface plasmon peak in Ga nanoparticle monolayers embedded in SiO_x matrix, as a function of the average particle radius R. The experimental points are obtained from the effective-medium analysis of linear transmittance curves. The frequency of the SH signal corresponds to 3.09 eV and is represented by the dashed line.

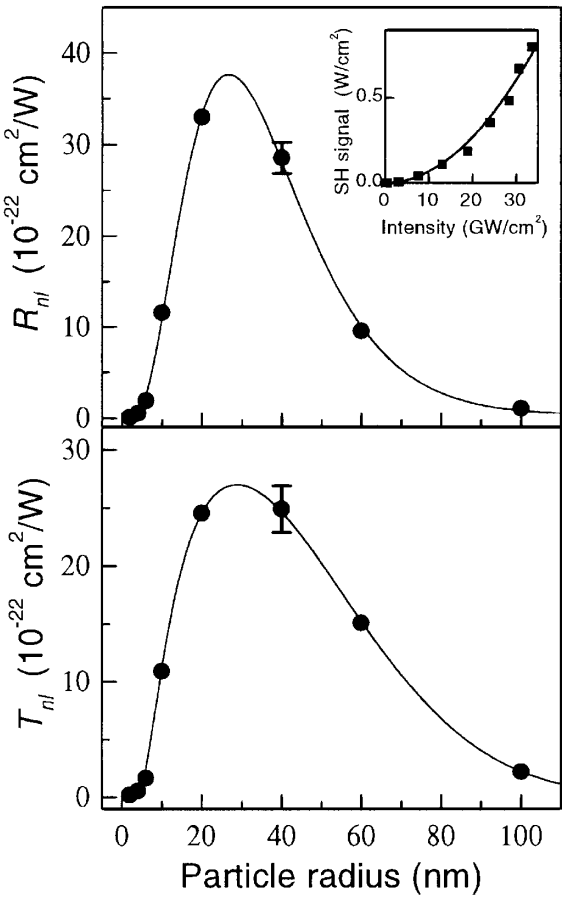

FIG. 2. Nonlinear reflection R_{nl} and transmission T_{nl} of different samples of Ga nanoparticle monolayers embedded in a SiO_x matrix, as a function of the average particle radius R. The SH signals are collected at normal incidence in transmission and at 2° in reflection. The continuous lines are guides for the eye. Typical error bars for R_{nl} and T_{nl} are indicated. Inset: Quadratic dependence of the SH signal on the incident flux.

transmittance at normal incidence, the temperature is then decreased down to LNT and raised back to 320 K at the same rate. A typical behavior of T_{nl} is illustrated in Fig. 3, where data averaged over 10 K are plotted for one of the samples exhibiting high SH efficiency, i.e., that with radius $R = 40$ nm. The curve has a quasisigmoidal shape illustrative of an hysteresis loop between 150 and 270 K, reproducing solidification and melting processes of the Ga nanoparticles occurring in this temperature range.

In detail, the behavior of T_{nl} during cooling from 300 to 160 K can be viewed as a decrease modified by a specific structure at 230 K. After the solidification drop between 150 and 140 K, the initial negative slope is then resumed down to 77 K. Conversely, during heating the SH signal exhibits a rather constant T_{nl} value till about 200 K. The SH signal then strongly increases forming an hysteresis loop which closes only at about 300 K. Along these positive slopes a structure about 255 K appears which is similar to the one observed at 230 K during cooling. We note that the undercooling process drives a sharp transition to the solid state. On the contrary, during heating, transitions to fully molten conditions extend on a broader temperature range (200–270 K), and are clearly size dependent. This asymmetric behavior has already been observed on a number of metallic nanoclusters in the linear response [11], and presents here some relevant details connected to the nature of the SH signal. In this respect the features between 230 and 255 K observed both during cooling and heating cycles should be related to solid-solid phase transitions of Ga nanoparticles [12]. The T_{nl} values give an increase of 40%–50% of the SH signal at $\lambda = 400$ nm during heating from 77 to 320 K. The corresponding increase in linear transmittance measured on the same sample amounts to less than 0.5%, when detected [13]. Therefore the SH hysteresis cycle is 80–100 times amplified with respect to the linear one. Melting and solidification were checked to follow similar hysteresis cycles down to nanoparticle radii of 10 nm. For smaller particles the area of the hysteresis cycle tends to vanish.

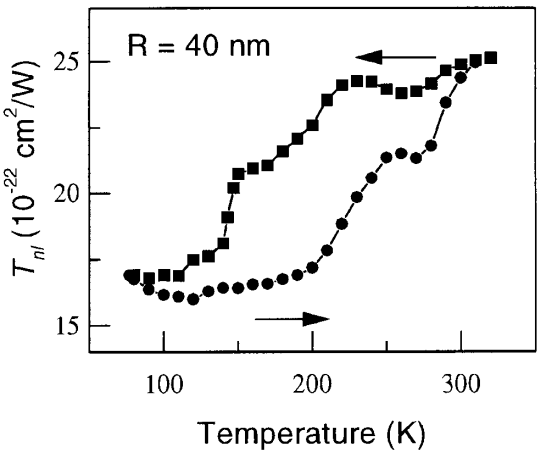

FIG. 3. Second-harmonic response of a Ga nanoparticle sample with 40 nm average radius upon cooling (squares) and heating (circles) cycles. Temperature measurements are performed by keeping the sample in a cold finger cryostat driven by a temperature controller in the range LNT–320 K with a scan rate of $\sim$2 K/min. The SH signals are collected at normal incidence in transmission and the exciting wavelength is $\lambda = 800$ nm.

A deeper insight into the behavior of the generated SH intensity with temperature can be gained by an estimate of the ratio of the liquid-to-solid SHG, using existing optical models and dielectric data for Ga and SiO_x from literature. It is well known from classical nonlinear optics [14] that for the case of composite materials the SH signal may be expressed in terms of local enhancement factors $Q(\omega)$, which account for the geometry of the nanoparticles, their optical response, as well as for the presence of a dielectric matrix. In this way one obtains for the ratio of the liquid (l) to solid (s) phase intensities

$$H = \frac{I_l^{2\omega}}{I_s^{2\omega}} = \frac{Q_l(2\omega)Q_l(\omega)^2}{Q_s(2\omega)Q_s(\omega)^2}. \quad (1)$$

The explicit form of $Q(\omega)$ is a function of material parameters such as dielectric functions of constituents, particle mean size, and effective-medium dielectric constants. In our case we adopt a Mie representation of the system to model the nonlinear interaction with the incident electromagnetic field [15].

A self-consistent estimate of the linear ''effective'' polarizability α_{eff} of Ga nanoparticles in both phases is obtained through an ''image-field model'' calculation [16]. α_{eff} values are determined by considering the dipoles formed by charges at the nanoparticle surface and their mirrored images in the matrix material. These charges are located at a distance from the metal/matrix interface limited by the screening depth of Ga (~ 0.8 Å). The effective polarizability is then calculated [17]. The resulting sudden change of α_{eff} at the solid-liquid phase transition is mainly due to (i) the vanishing of the electronic interband transitions, giving rise to a large variation of the dielectric function at melting (e.g., +50% at $\lambda = 400$ nm) [18–20], (ii) the mass density increasing by 3.2% upon melting [21], and (iii) the free-electron density of liquid Ga which is assumed 0.6 times the solid value [12]. Through the Maxwell-Garnett approach the effective-medium dielectric constants at ω and 2ω frequencies to be used in the Mie formulas are finally derived, and the estimated $Q(\omega)$ and H values are obtained. The calculation gives $H = 2.4 \pm 0.5$, the uncertainty being ascribed only to the spread in dielectric function values found in the literature. Such a value is compared to the experimental value $H = 1.5 \pm 0.2$ (by considering the error bars) obtained by the ratio of SH values of liquid-to solid nanoparticles at 300 and 77 K, respectively. Within the above specified parameter dependence of H, the calculated value of H might be brought to a closer agreement with the experimental value by

employing more refined effective-medium models, e.g., taking into account the interactions between closed packed nanoparticles. These models in turn depend critically on the deviations of the size dependent dielectric functions from their bulk values, a nontrivial task for future work.

It should be noted that in principle this analysis can be extended to the nonlinear response of Ga nanoparticles across phase transitions different from melting, i.e., solid-solid ones, although the variations of the effective polarizability are expected to be less pronounced. While the maximum variation in mass density across the δ to β solid phase transition is 0.5% [21], the changes in the dielectric function and free-electron density (which are not available in the literature) may be smaller than in the melting case. This analysis is useful to account for the details of the hysteresis cycle reported in Fig. 3. In fact, melting of Ga nanoparticles is known to initiate with the formation of a liquid layer around the solid core [7]. The melt front propagates inwards on a broad temperature interval, until $\sim$260 K where the average nanoparticle distribution melts. Moreover, in a temperature range below 260 K the solid Ga nuclei are known to undergo solid-solid phase transitions from γ or δ phases to the β phase [12]. The sudden changes in dielectric functions and densities taking place at these transitions determine corresponding structures in the SH intensity, which are clearly more relevant than in the linear response. The SH signal reaches the initial levels around 300 K, where all nanoparticles, whatever their phase and size, are completely molten.

In summary, through second-harmonic generation we have observed an amplified hysteresis curve for Ga nanoparticles across the solid-liquid phase transition, which could be of relevance for diagnostic purposes in nanometric systems. The nonlinear emission has been optimized by selecting the second-harmonic wavelength in resonance with the surface plasmon of the nanoparticles. For the specific case of Ga an amplification factor of 2 orders of magnitude is observed in the ratio of the melting-induced enhancement of the SH signal with respect to the linear response at the same wavelength. The model analysis here introduced illustrates the key role of parameters like mass density, dielectric function, and free-carrier concentration, in determining the SH amplification. In principle, with a suitable choice of materials and phase transitions, this amplification factor of the nonlinear signal can be governed and changed in a wider range, thus reaching levels of interest for applications.

The authors acknowledge the financial support of Progetto Finalizzato CNR-MADESS II and the use of the laser source from the INFM-ELPHOS project.

[1] N. Bloembergen, Appl. Phys. B **68**, 289–293 (1999).
[2] H. J. Simon, D. E. Mitchell, and J. G. Watson, Phys. Rev. Lett. **33**, 1531 (1974).
[3] D. Ricard, P. Roussignol, and C. Flytzanis, Opt. Lett. **10**, 511 (1985); A. Brysch, G. Bour, R. Neuendorf, and U. Kreibig, Appl. Phys. B **68**, 447 (1999).
[4] G. T. Boyd, T. Rasing, J. R. Leite, and Y. R. Shen, Phys. Rev. B **30**, 519 (1984).
[5] E. Søndergård, R. Kofman, P. Cheyssac, and A. Stella, Surf. Sci. **364**, 467 (1996).
[6] D. Chatain, I. Rivollet, and N. Eustathopoulos, J. Chim. Phys. Phys.-Chim. Biol. **84**, 201 (1987).
[7] Y. Lereah, R. Kofman, J. J. Penisson, G. Deutscher, P. Cheyssac, T. Ben David, and A. Bourret, Philos. Mag. B **81**, 1801 (2001).
[8] P. Tognini, A. Stella, P. Cheyssac, and R. Kofman, J. Non-Cryst. Solids **249**, 117 (1999).
[9] M. Falasconi, L. C. Andreani, A. M. Malvezzi, M. Patrini, V. Mulloni, and L. Pavesi, Surf. Sci. **481**, 105 (2001).
[10] A. M. Malvezzi, M. Patrini, A. Stella, P. Tognini, P. Cheyssac, and R. Kofman, Eur. Phys. J. D **16**, 321 (2001).
[11] R. Kofman, P. Cheyssac, and R. Garrigos, Phase Transit. **24-26**, 283 (1990).
[12] A. Defrain, J. Chim. Phys. Phys.-Chim. Biol. **74**, 851 (1977).
[13] M. Nisoli, S. Stagira, S. De Silvestri, A. Stella, P. Tognini, P. Cheyssac, and R. Kofman, Phys. Rev. Lett. **78**, 3575 (1997).
[14] C. K. Chen, T. R. Heinz, D. Ricard, and Y. R. Shen, Phys. Rev. B **27**, 1965 (1983).
[15] T. Müller, P. H. Vaccaro, F. Balzer, and H.-G. Rubahn, Opt. Commun. **135**, 103 (1997).
[16] J. D. Jackson, *Classical Electrodynamics* (John Wiley & Sons, New York, 1999), 3rd ed.
[17] F. W. King, R. P. Van Duyne, and G. C. Schatz, J. Chem. Phys. **69**, 4472 (1978).
[18] P. De la Bretèque, Bulletin d'Information et de Bibliographie **88**, 60 (1970).
[19] G. Hass and L. Hadley, in *American Institute of Physics Handbook*, edited by D.E. Gray (McGraw-Hill, New York, 1972), 3rd ed.
[20] R. Kofman, P. Cheyssac, and J. Richard, Phys. Rev. B **16**, 5216 (1977).
[21] A. Di Cicco, Phys. Rev. Lett. **81**, 2942 (1998).